

Low-Cost Optoacoustic Tomography System with Programmable Acoustic Delay-Line

Daohuai Jiang, Hengrong Lan, Yiyun Wang, Feng Gao, and Fei Gao, *Member, IEEE*

Abstract—Photoacoustic tomography (PAT) is an emerging technology for biomedical imaging that combines the superiorities of high optical contrast and acoustic penetration. In the PAT system, more photoacoustic (PA) signals are preferred to be detected from full field of view to reconstruct PA images with higher fidelity. However, the requirement for more PA signals' detection leads to more time consumption for single-channel scanning based PAT system, or higher cost of data acquisition (DAQ) module for an array-based PAT system. To address this issue, we proposed a programmable acoustic delay line module to reduce DAQ cost and accelerate imaging speed for PAT system. The module is based on bidirectional conversion between acoustic signals and electrical signals, including ultrasound transmission in between to provide sufficient time delay. The acoustic delay line module achieves tens or hundreds of microseconds' delay for each channel, and is controlled by a programmable control unit. In this work, it achieves to merge four inputs of PA signals into one output signal, which can be recovered into original four PA signals in the digital domain after DAQ. The imaging experiments of pencil leads embedded in agar phantom is conducted by the PAT system equipped with the proposed programmable acoustic delay-line module, which demonstrated its feasibility in biomedical imaging system.

Index Terms—Acoustic delay line, programmable delay line, low cost, optoacoustic tomography, signal recover

I. INTRODUCTION

Photoacoustic tomography (PAT), as a kind of emerging noninvasive imaging modality, has shown its unique advantages in biomedical imaging, combining the strength of both deep penetration of ultrasound wave and high contrast of optical absorption [1-5]. In a conventional PAT system, after excitation of a laser pulse, an ultrasonic transducer array will receive the PA signals from different directions and reconstruct the PA image from these PA signals [6]. The more PA signals acquired for image reconstruction, the less distortion and artifacts for the reconstructed PA image. To accelerate the PAT imaging speed or get more PA signals at one laser shot, the ultrasound array with more elements is applied for PA signals

detection in the PAT system [7-9]. However, more PA signals' detection will consume more high-speed data acquisition (DAQ) channels, leading to dramatic cost increase for PAT system [10].

For a full-ring ultrasound transducer array-based PAT system, the useful PA signal length depends on the diameter of the ring transducer. It is interesting to observe that the PA signals' durations are usually less than 40 microseconds (assuming that the velocity of the PA wave is 1500 m/s and the diameter is 60 mm, then $t=(60mm)/(1500m/s)=40\mu s$) with laser pulse repetition rate of 20 Hz, which means that the time interval between two PA signals is about 50 milliseconds [11]. Therefore, it turns out that for most of the operating time (1-40 μs /50ms = 99.92%), the status of DAQ is idle. Fig. 1(a) shows that the conventional PA signal sampling method with PA signal connecting with DAQ one by one, whose DAQ work status is shown in Fig. 1(c). In each pulse cycle, one channel of DAQ only samples one PA signal, and for most of the time in one cycle, DAQ works at idle status. To utilize the DAQ's capability more efficiently and reduce the number of acquisition channels for PA signals' sampling, we proposed the method of time-sharing multiplexing for PA signals sampling by applying a custom-designed programmable acoustic delay-line (PADL) module in this paper. Fig. 1(b) shows the n -in-1 data sampling method with n -in-1 PADL module, where n channels' PA signals are sampled only by single channel DAQ. Fig. 1(d) shows the DAQ working status: at one pulse cycle, one channel of the DAQ can sample n channels' PA signals with n times higher use efficiency.

The time-sharing multiplexing method depends on the realization of analog signals' time delay. Murat Kaya Yapici, et al proposed a parallel acoustic delay line for PAT based on the detection and ultrasound transmission by optical fiber, which however suffers limited sensitivity and bandwidth [12, 13]. The delay line module based on capacitor storage in [14] is complex for delayed signals' recovery. To realize tens or hundreds of microseconds' time delay for analog signal, the mostly used method is via the acoustic wave propagation. The acoustic wave that travels at velocity v at a distance d gives $t_d=d/v$ time delay

This research was funded by Natural Science Foundation of Shanghai (18ZR1425000), and National Natural Science Foundation of China (61805139). (Corresponding author: Fei Gao.)

Daohuai Jiang (e-mail: jiangdh1@shanghaitech.edu.cn), Hengrong Lan (e-mail: lanhr@shanghaitech.edu.cn) and Yiyun Wang (e-mail: wangyy@shanghaitech.edu.cn) are with the Hybrid Imaging System Laboratory (HISLab), Shanghai Engineering Research Center of Intelligent Vision and Imaging, School of Information Science and Technology, ShanghaiTech University, Shanghai 201210, China, with Chinese Academy of

Sciences, Shanghai Institute of Microsystem and Information Technology, Shanghai 200050, China, and also with University of Chinese Academy of Sciences, Beijing 100049, China.

Feng Gao and Fei Gao are with the Hybrid Imaging System Laboratory (HISLab), Shanghai Engineering Research Center of Intelligent Vision and Imaging, School of Information Science and Technology, ShanghaiTech University, Shanghai 201210, China (e-mail: gaofeng@shanghaitech.edu.cn, gaofei@shanghaitech.edu.cn).

[15]. Generally speaking, the requirements for a dedicated acoustic delay line module include low acoustic attenuation over a wide bandwidth, smaller velocity (smaller size for same delay time), easy signal recovery after propagation, proper signal amplitude compensation, compatibility for different transducer types, etc.

methodology of the delay line module including the general wave extrapolation and delayed signal recover method. In section III, a PAT system based on the PADL module will be introduced, and a pencil leads made phantom is imaged to verify the feasibility of the delay line module. Section IV presents discussions and conclusions for the PADL module based PAT system.

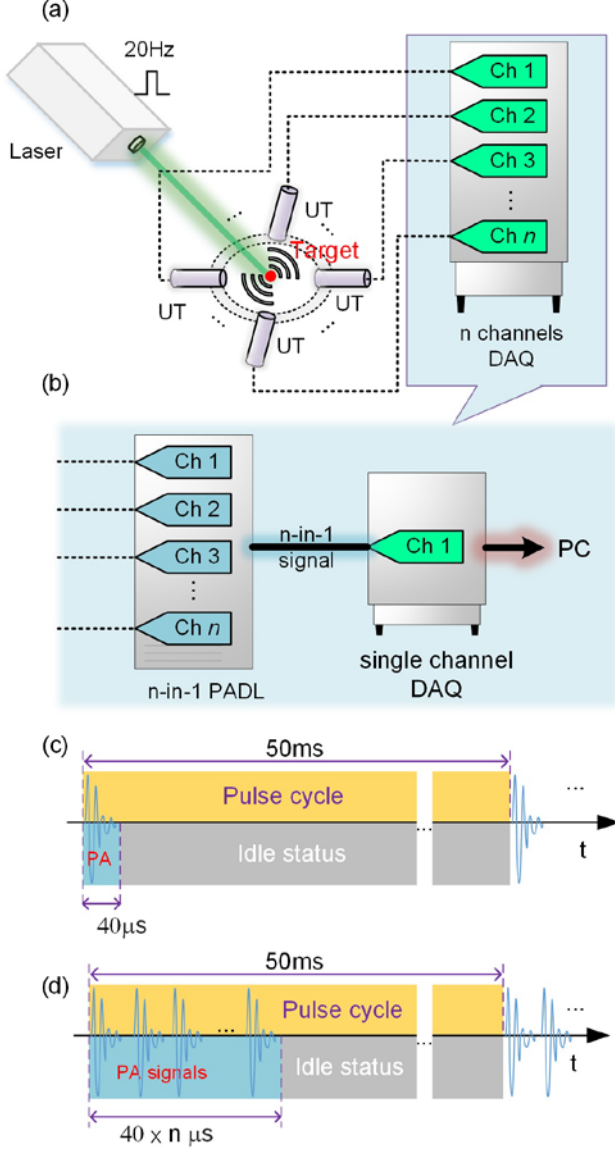


Fig. 1. The PA signals sampling setup with (a) conventional method and (b) time-sharing multiplexing by a PADL module; (c) and (d) are the DAQ working status corresponding to (a) and (b) setup. UT: ultrasound transducer; DAQ: data acquisition; PADL: programmable acoustic delay-line; PC: personal computer.

In this paper, to address the abovementioned issues, we proposed a four-in-one programmable acoustic delay-line (PADL) module for PA signal acquisition. This module can achieve time delay ranging from tens to hundreds of microseconds, including a programmable unit to achieve different time delays. By exactly recovering the original PA signals without time delay, image reconstruction will be performed in the digital domain after DAQ sampling.

This paper is organized as follows: Section II presents the

II. PROGRAMMABLE ACOUSTIC DELAY-LINE

The method of reducing DAQ cost for PAT system is based on the delay line module to delay the signals in analog domain and recover the signals after sampling in digital domain. In this section, we will introduce the programmable acoustic delay line module, the general wave extrapolation and delayed signal recovery method primarily.

A. PA Physical Theory

The PA wave equation is shown below describing the PA wave propagation in both time and spatial domains [16, 17]:

$$\left(\nabla^2 - \frac{1}{c^2} \frac{\partial^2}{\partial t^2} \right) p(r, t) = 0 \quad (1)$$

subject to the initial conditions:

$$p(r, t)|_{t=0} = \frac{\beta c^2}{C_p} A(r); \quad \frac{\partial p(r, t)}{\partial t}|_{t=0} = 0, \quad (2)$$

where ∇^2 denotes the Laplacian operator, and $A(\mathbf{r})$ is the distribution of absorbed optical energy density. The constants β , c and C_p denote the thermal coefficient of volume expansion, speed of sound and the specific heat capacity of the medium at constant pressure, respectively. Assuming that the received photoacoustic wave is $p(r, t)$, the PA image is reconstructed by PA signals which reflect the $p(r, t)$ information [18]. The relationship of delayed PA signals we received and $p(r, t)$ function can be regarded as:

$$s(i, t + t_d) \propto p(r, t + t_d) \quad (3)$$

where $p(r, t + t_d)$ is delay acoustic pressure corresponding to i^{th} delayed PA signal $s(i, t + t_d)$, t_d is delay time. The delayed signal $s(i, t + t_d)$ can be recovered into $s(i, t)$ without time delay. Moreover, the signal $s(i, t)$ is corresponding to the acoustic pressure of $p(r, t)$. Hence, with proper data processing, the delay signals $s(i, t + t_d)$ can also reconstruct the PA image.

B. Delay-line Design and Implementation

Achieving nanoseconds' time delay for analog signal is available by extended electric wire or by some commercial integrated chip. However, the PA signal's duration is dozens of microseconds, which requires at least tens or hundreds of microseconds' delay time for the time-division multiplexing sampling method. However, the conventional method based on electrical or optical signal time delay is difficult to achieve tens

of microseconds' level [14]. On the other hand, the acoustic propagation velocity is several orders of magnitude slower than the speed of electrons. Therefore, we propose to transform the electrical analog signal to acoustic signal, which can easily achieve tens or hundreds of microseconds time delay. Fig. 2 shows the 4-in-1 programmable acoustic delay-line module.

The acoustic delay-line unit is based on bidirectional conversion between acoustic signals and electrical signals. Two ultrasound transducers are used for signal conversion, one for signal transmitting and one for receiving. We selected purified water as the acoustic transmission medium, and the acoustic speed in the water at room temperature (25°C) is about 1.5 mm/ μ s [17, 19]. It deserves noting that water gives less acoustic attenuation and better coupling with the ultrasound transducer. Fig. 2(a) shows the water-made acoustic delay-line structure and its photograph. The distance between two ultrasound transducers is 60 mm, which corresponds to 40 μ s time delay ((60mm)/(1.5mm/ μ s)=40 μ s). A transparent polyvinyl chloride (PVC) tube is used to seal water in it. The external diameter of the PVC tube is 15 millimeters and the internal diameter is 13 millimeters. Besides, it is noticed that the PVC tube is fully filled with purified water without air to make better acoustic coupling and propagation.

The above-mentioned delay-line unit in Fig. 2(a) can only achieve a fixed time delay (40 μ s), which is insufficient for multi-channel data acquisition that requires different time delays for each channel. To address this issue, based on the delay-line unit, we designed the PADL unit, which can realize programmable time delay. Fig. 2(b) shows the structure and its signal transmission diagram. The acoustic delay-line unit is the basics of the PADL, and three analog switches are used to implement signal control. Besides, a low noise pre-amplifier (LNPAmp) and a variable gain amplifier (VGamp) are used to compensate for the delayed signal's attenuation. An analog adder connects the delayed signal and delay-line unit input that constitutes close-loop feedback, within which PA signal can run repeatedly to achieve enough time delay (multiple of 40 μ s). The three analog switches controlling signal input, signal output and signal feedback are corresponding to SW_{in} , SW_{out} and SW_{fb} in the figure, respectively. Besides, the analog switches controlling logics are generated by a field-programmable gate array (FPGA) with a particularly designed time sequence. To make sure the feedback loop works stable, the loop gain including LNPAmp and VGamp should be less than one.

The schematic diagram of the 4-in-1 delay-line module is shown in Fig. 2(c). The module includes three delay units (1,2, and 3) based on the proposed PADL module, and a transfer unit (T unit) that consists of resistors network. The signal input to T unit experiences no time delay, but the resistor network adjusts the amplitude, and an analog switch (SW_{out}) controls the signal output. Moreover, the other three input signals go through delay units with different time delays. In addition, a four-in-one analog adder combines the four signals into one output. Hence, the four parallel pulse inputs are converted into one pulse train with efficient time intervals, so that the four inputs have no aliasing, then it is able to be recovered into four signals after DAQ sampling in the digital domain.

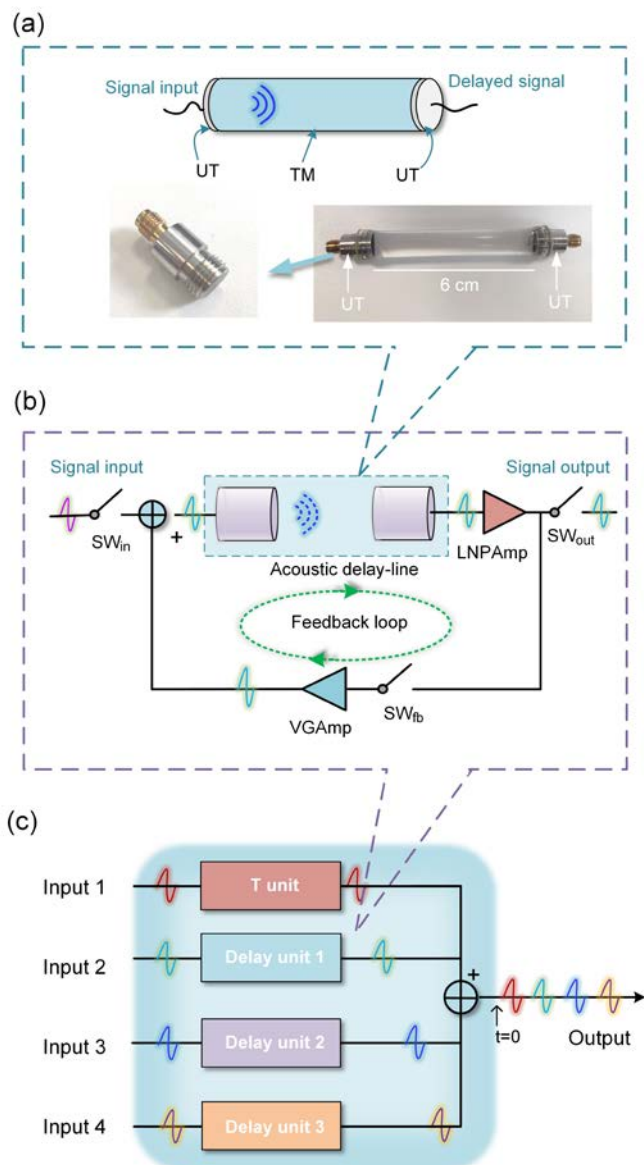


Fig. 2. The structure of the 4-in-1 programmable acoustic delay-line module. (a) the acoustic delay-line unit structure, and its photograph; (b) the schematic of the programmable acoustic delay-line unit; (c) the schematic diagram of the 4-in-1 PADL delay-line module. UT: ultrasound transducer; TM: transmission medium; SW: switch; LNPAmp: low noise pre-amplifier; VGamp: variable gain amplifier; T unit: transfer unit.

The acoustic delay-line signal transfer characteristics is tested and shown in Fig. 3. Fig. 3(a) shows the acoustic signal waveforms before and after an acoustic delay-line unit. The red curve is the input PA signal detected by the ultrasound transducer. The delayed signal (blue curve) gone through the delay-line achieves 40 μ s time delay and amplitude attenuation. The waveform of the output is highly correlated with input signal's waveform. Fig. 3(b) shows acoustic delay-line transfer characteristics with multi-cycle loops. The red curve is the input of the PADL module, and the blue curve of a pulse train is delayed signal output at different cycles. Each pulse of the output signal has interval of 40 μ s, so that we can selectively achieve the total delay time by setting proper cycle number.

Except time delay, the PADL module also induces amplitude attenuation that has to be compensated. Fig. 3(c) shows the delayed signal amplitude attenuation, which is related with the distance between two UT and feedback loop cycles. In this design, the selected PVC tube is 60 mm long that causes acoustic attenuation of about 41 dB. The blue star-labeled line stands for the feedback loop cycles caused attenuation, which almost can be neglected.

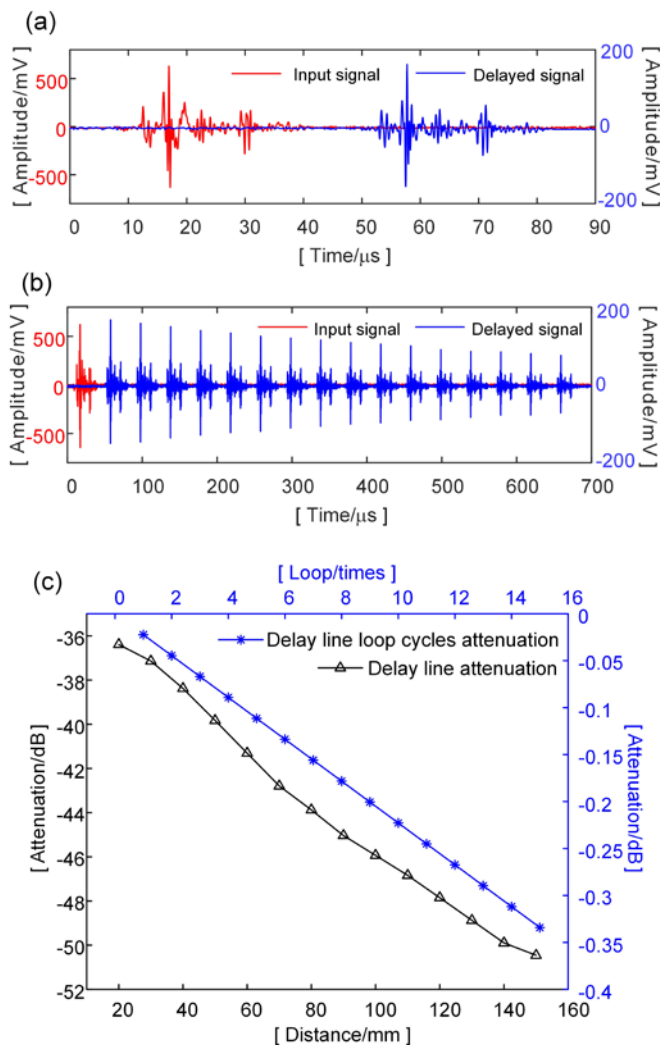


Fig. 3. The signal transfer characteristics of the programmable acoustic delay-line module. (a) acoustic delay-line transfer characteristics of PA signals; (b) acoustic delay-line transfer characteristics with multi-cycle loops; (c) acoustic delay-line signal attenuation characteristics related with UT distance and cycle number.

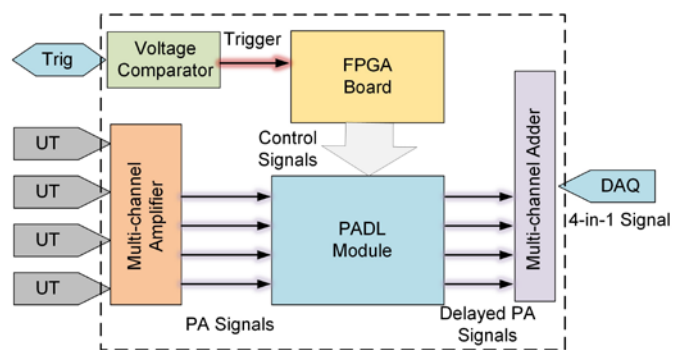


Fig. 4. The 4-in-1 PADL module implementation. Trig: laser trigger; FPGA: field-programmable gate array; UT: ultrasound transducer; PA: photoacoustic; PADL: programmable acoustic delay-line; DAQ: data acquisition device.

C. Four-in-one PADL Module Design and Implementation

The 4-in-1 PADL module contains five parts: multi-channel amplifier, voltage comparator, FPGA board, PADL and multi-channel adder as shown in Fig. 4. The voltage comparator is used for laser trigger detection that generates a trigger signal shown in Fig. 5(a), to FPGA for controlling the PADL. Besides, the FPGA board generates specific control logics to the analog switches of the PADL as shown in Fig. 5(c). The PADL delays the UT detected pre-amplified PA signals, and all the delayed signals enter into the multi-channel adder to generate the 4-in-1 delayed signal that is captured by DAQ.

As shown in previous Fig. 2(b), the analog switches SW_{in} , SW_{out} and SW_{fb} control the delay time of the PADL. To achieve different time delay by the 4-in-1 delay-line module, we need to control 10 analog switches in total: a switch for T unit and 3 switches for each delay-line unit. Fig. 5 shows the 4-in-1 PADL module control logic and its corresponding delayed PA signals. Fig. 5(a) is the laser trigger signal: the laser is triggered at the rising edge t_0 . Fig. 5(b) shows the four PA signals detected by UTs. The detected signals are disturbed by a strong electromagnetic coupling interference signal at t_0 , which is useless for PA image reconstructions. Hence, the delayed PA signal should exclude the coupling interference signals, so the SW_{in} needs to be closed at t_1 that is after t_0 and before PA signal comes in. Fig. 5(c) shows the analog switches control logics. Delay units signal inputs switch SW_{in} and T unit output switch SW_{out} are closed from t_1 to t_2 that covers the duration containing PA signals, and output the no-delay PA signal (PA1). The delay unit 1 output switch SW_{out1} is closed from t_2 to t_3 , so that it outputs one-cycle delayed signal (PA2). For the delay unit 2, the feedback switch $SW_{fb} Unit2$ is closed from t_2 to t_3 and the output switch SW_{out2} is closed from t_3 to t_4 , so that it outputs two-cycles delayed signal (PA3). The delay unit 3 feedback switch $SW_{fb} Unit3$ is closed from t_2 to t_4 and the output switch SW_{out3} is closed from t_4 to t_5 , so that it outputs 3-cycles delayed signal (PA4). Fig. 5(d) shows delayed signals' outputs, the blue (PA1), red (PA2), yellow (PA3) and purple (PA4) from the up to down correspond to the output of T Unit, Delay Unit 1, Delay Unit 2 and Delay Unit 3 in Fig. 2(c), respectively. After we get PA signals with different time delays that is long enough to separate these signals in time domain, the multi-channel analog

adder combines the four delayed signals into one output. Fig. 5(e) shows the 4-in-1 delayed signals, where the parallel 4 inputs are converted into a serial output. Therefore, by applying the 4-in-1 PADL module, a one-channel DAQ device is available to capture 4 channels' PA signals at one laser shot.

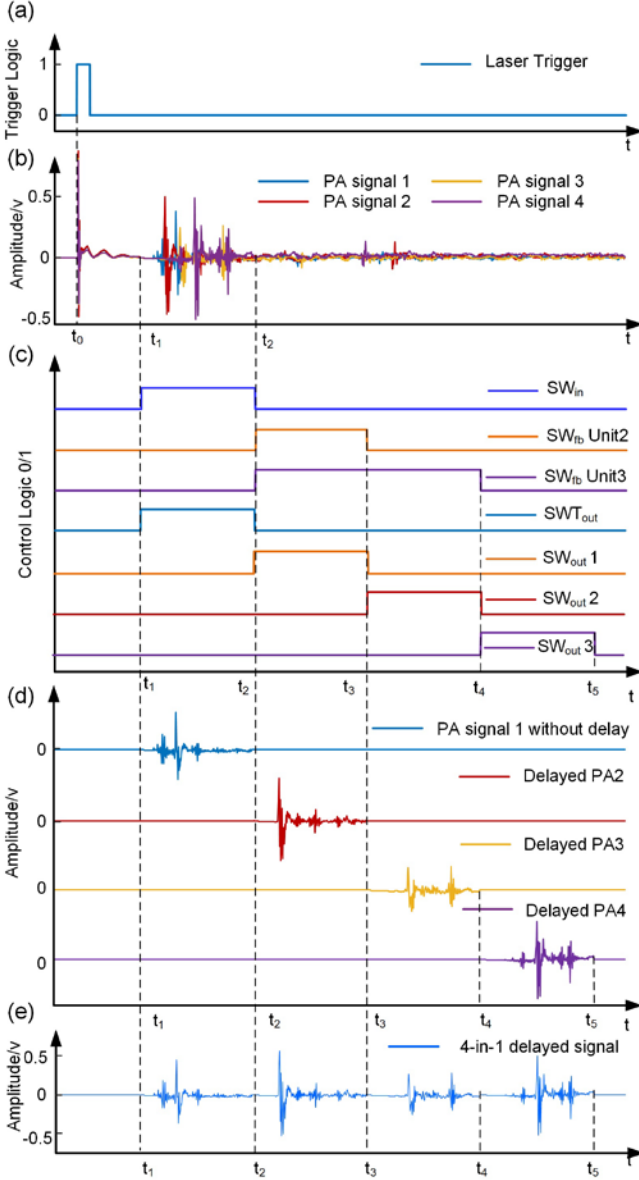


Fig. 5. The 4-in-1 PADL module's control logic waveforms and its corresponding delayed signals and 4-in-1 signal. (a) laser trigger signal; (b) PA signals; (c) the PDLA control logic; (d) delayed signal outputs; (e) the delayed 4-in-1 signal;

D. Delayed Signal Recovery

After we get the 4-in-1 delayed signal, it is feasible to recover the delayed signal into four separate PA signals in digital domain. The signal recovery process in digital domain is the reverse operation of the signal delay in analog domain [20]. Fig. 6 shows the diagram of the 4-in-1 signal' delay and recovery processing. The operation of signal summation, time delay and amplification in analog domain are corresponding to the signal separation, time shift and magnification in digital domain.

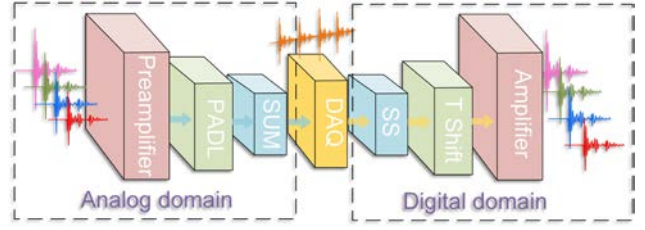


Fig. 6. The diagram of four-in-one signals' delay and recovery processing. PADL: programmable acoustic delay-line module; SUM: summation; DAQ: data acquisition; SS: signal separation; T shift: time shift transform.

The PADL module transferring 4 PA signals with different time delays also induces different amplitude attenuations shown in Fig. 3(c). The signal magnification in digital domain should compensate for this amplitude attenuation. For the signal delay part, the parallel inputs are firstly transformed into a serial signal and sampled by DAQ. After sampling, the 4-in-1 signal should be separated into four parts according to their different delay times, respectively. The parallel input signals and the delayed signal follow below equation:

$$s(t+t_{di}) = A_i \cdot \sum_{i=1}^4 \bar{s}(i,t) \cdot k(i,\bar{s}) \quad (4)$$

where $s(t+t_{di})$ is delayed signal, t_{di} stands for channel i delayed time of the 4-in-1 PADL module. $\bar{s}(i,t)$ is the parallel input signals, where i ranges from 1 to 4. $k(i,s)$ is a transfer function of a bandpass filter, which is due to the limited bandwidth of UT's bidirectional conversion between acoustic signals and electrical signals of the delay-line module. A_i is the acoustic signals attenuation coefficient and it is determined by:

$$A_i = A_p \cdot A_l \cdot A_m \quad (5)$$

where A_m is the loop gain of each delay-line units. A_p and A_l are acoustic signal attenuation coefficients corresponding to acoustic propagation distance and feedback loops, respectively. A_p can be calculated by the formula below:

$$p_x = p_0 e^{-\alpha f x} = p_0 \cdot A_p \quad (6)$$

where p_x is the ultrasound amplitude received at a distance x , p_0 is the ultrasound amplitude at the transmit UT, α is acoustic attenuation coefficient, f is the frequency of the ultrasound signal. To simplify the expression, we define $A_p = \exp(-\alpha f x)$ for each channel of the delay line module.

Based on Eq. (4), we can get the related expression in the digital domain:

$$S[n+q_i] = A_i \cdot \sum_{i=1}^4 \bar{S}[i,n_i] \cdot K[i,\bar{S}] \quad (7)$$

$$n = \{1, 2, 3, \dots, S_n - q_4\}, n_i = \{1, 2, 3, \dots, N_i\}$$

where $S[n+q_i]$ is data of the delayed signal and the data length is S_n , n ranges from 1 to $S_n - q_4$ (q_4 is data length corresponding

by applying the proposed method, we can get the recovered PA signals after removing time delay. Fig. 8(b)-(e) show recovered PA signals from one of the 4-in-1 delayed signals, which will be used for image reconstruction.

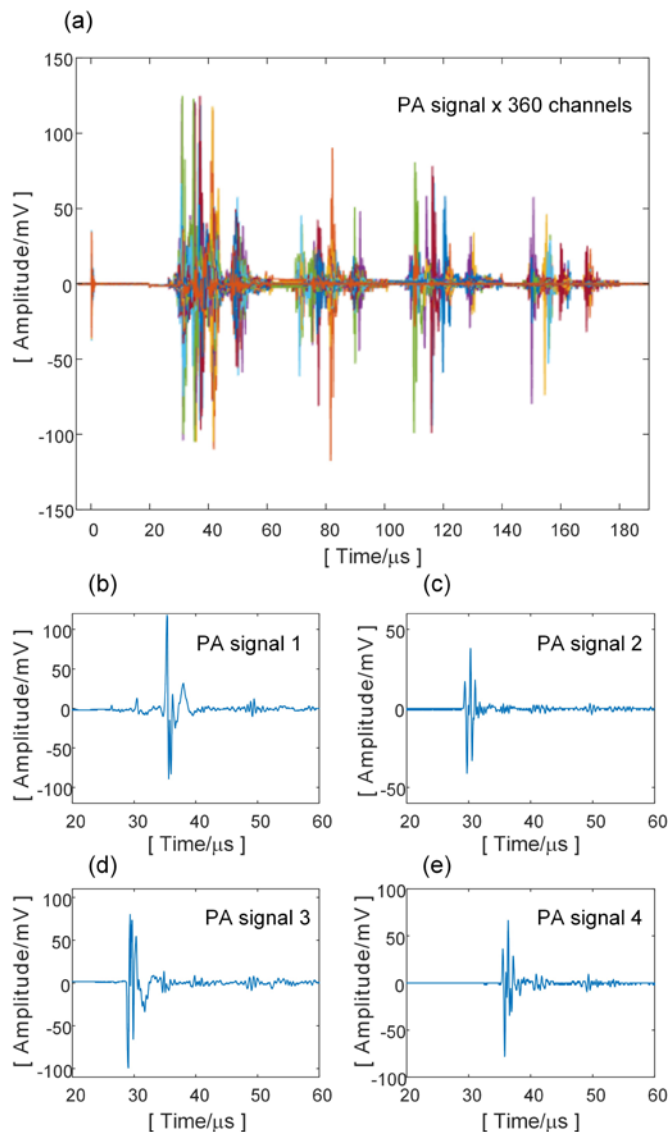


Fig. 8. The 4-in-1 delayed PA signals and recovered PA signals. (a) 360 channels of 4-in-1 delayed PA signals; (b), (c), (d) and (e) is a group of recovered PA signals corresponding to one of 4-in-1 delayed signals.

C. Imaging Result

To demonstrate the feasibility of the 4-in-1 PADL module integrated in the PAT system, we have imaged a pencil leads made phantom with both the traditional sampling method and the proposed sampling method using the 4-in-1 PADL module. The phantom is made up of three crossed 0.5 mm diameter pencil leads embedded in an agar block with inclination. Fig. 9(a) shows the photograph of phantom in top view, whose profile is like a triangle. Moreover, Fig. 9(b) is the photograph of the phantom in lateral view showing the imaging target in different depth, where the white dotted circles indicate the corresponding part between Fig. 9(a) and (b). Fig. 9(c) shows the PAT imaging result by conventional method, and Fig. 9(d) is the imaging result using 4-in-1 delayed signals based PAT image reconstruction. The image reconstruction is implemented

in *MATLAB 2018b* version with the classical back-projection algorithm [21, 22]. Both Fig. 9(c) and (d) show the detailed structure of the phantom. The dotted line circled in the phantom is the pencil leads embedded deeper in the agar block, which shows weaker PA signal due to more acoustic attenuation. Overall, it shows that the delayed signals suffers negligible distortion and achieve even better imaging results with lower system cost than conventional method.

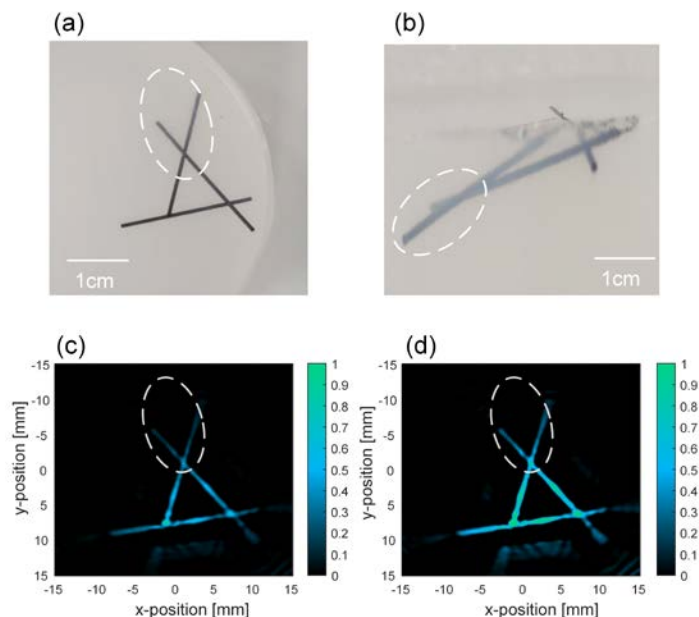


Fig. 9. (a) the top view of the phantom; (b) the lateral view of the phantom; (c) the PAT imaging result with conventional signals sampling method; (d) the PAT imaging result with 4-in-1 PADL module sampling method.

IV. CONCLUSION

In this paper, the proposed 4-in-1 PADL module achieves programmable time delay for the PA signals ranging from tens to hundreds of microseconds. Moreover, the FPGA board can conveniently tune the delay time of the PADL module. The delayed signal is restorable in the digital domain with the proposed method according to the delay-line module. By applying the module, one channel DAQ can sample four PA signals concurrently. The PAT system integrated with the 4-in-1 PADL module can reduce the system cost and accelerate imaging speed. By the phantom imaging experiments, the feasibility of the PADL module is well demonstrated. This work provides a potential method to significantly reduce the cost and accelerate the imaging speed of the PAT system[23]. Furthermore, the 4-in-1 PADL module is also appropriate for other kinds of pulse signals' time delay beyond ultrasound. The demonstrated PAT system in this paper, which is based on the 4-in-1 PADL module, has reduced 75% of the DAQ cost or reduced the time consumption of the PAT imaging. By applying more delay line units, the PADL module can merge more pulse signals into one delayed signal that can further reduce the system cost for real-time PA imaging system development.

V. ACKNOWLEDGMENT

This work was supported by the Natural Science Foundation of Shanghai (18ZR1425000) and the National Natural Science Foundation of China (NSFC) (61805139).

REFERENCES

- [1] L. V. Wang, "Tutorial on Photoacoustic Microscopy and Computed Tomography," *IEEE Journal of Selected Topics in Quantum Electronics*, vol. 14, no. 1, pp. 171-179, 2008.
- [2] Y. Zhou, J. Yao, and L. V. Wang, "Tutorial on photoacoustic tomography," *J Biomed Opt*, vol. 21, no. 6, p. 61007, Jun 2016.
- [3] L. V. Wang and S. Hu, "Photoacoustic tomography: in vivo imaging from organelles to organs," *Science*, vol. 335, no. 6075, pp. 1458-62, Mar 23 2012.
- [4] L. V. Wang and J. Yao, "A practical guide to photoacoustic tomography in the life sciences," *Nat Methods*, vol. 13, no. 8, pp. 627-38, Jul 28 2016.
- [5] J. Xia and L. V. Wang, "Small-animal whole-body photoacoustic tomography: a review," *IEEE Trans Biomed Eng*, vol. 61, no. 5, pp. 1380-9, May 2014.
- [6] P. K. Upputuri and M. Pramanik, "Recent advances toward preclinical and clinical translation of photoacoustic tomography: a review," *J Biomed Opt*, vol. 22, no. 4, p. 41006, Apr 1 2017.
- [7] A. A. Oraevsky *et al.*, "A fast 512-element ring array photoacoustic imaging system for small animals," presented at the Photons Plus Ultrasound: Imaging and Sensing 2009, 2009.
- [8] J. Xia, C. Huang, K. Maslov, M. A. Anastasio, and L. V. Wang, "Enhancement of photoacoustic tomography by ultrasonic computed tomography based on optical excitation of elements of a full-ring transducer array," *Opt Lett*, vol. 38, no. 16, pp. 3140-3, Aug 15 2013.
- [9] V. Ntziachristos, R. Zemp, G. Paltauf, P. Hartmair, G. Kovachev, and R. Nuster, "Photoacoustic tomography with a line detector array," presented at the Opto-Acoustic Methods and Applications in Biophotonics III, 2017.
- [10] H. Zhong, T. Duan, H. Lan, M. Zhou, and F. Gao, "Review of Low-Cost Photoacoustic Sensing and Imaging Based on Laser Diode and Light-Emitting Diode," *Sensors (Basel)*, vol. 18, no. 7, Jul 13 2018.
- [11] M. Xu and L. V. Wang, "Photoacoustic imaging in biomedicine," *Review of Scientific Instruments*, vol. 77, no. 4, 2006.
- [12] Y. Cho *et al.*, "Handheld photoacoustic tomography probe built using optical-fiber parallel acoustic delay lines," *J Biomed Opt*, vol. 19, no. 8, p. 086007, Aug 2014.
- [13] M. K. Yapici *et al.*, "Parallel acoustic delay lines for photoacoustic tomography," *J Biomed Opt*, vol. 17, no. 11, p. 116019, Nov 2012.
- [14] D. Jiang, H. Lan, H. Zhong, Y. Zhao, H. Li, and F. Gao, "Low-Cost Photoacoustic Tomography System Based on Multi-Channel Delay-Line Module," *IEEE Transactions on Circuits and Systems II: Express Briefs*, vol. 66, no. 5, pp. 778-782, 2019.
- [15] Z. Zhang, Y. Tian, Y. Cheng, Q. Wei, X. Liu, and J. Christensen, "Topological Acoustic Delay Line," (in English), *Physical Review Applied*, vol. 9, no. 3, Mar 28 2018.
- [16] K. Wang and M. A. Anastasio, "A simple Fourier transform-based reconstruction formula for photoacoustic computed tomography with a circular or spherical measurement geometry," *Phys Med Biol*, vol. 57, no. 23, pp. N493-9, Dec 7 2012.
- [17] C. Li and L. V. Wang, "Photoacoustic tomography and sensing in biomedicine," *Phys Med Biol*, vol. 54, no. 19, pp. R59-97, Oct 7 2009.
- [18] H. Jin *et al.*, "Pre-migration: A General Extension for Photoacoustic Imaging Reconstruction," *IEEE Transactions on Computational Imaging*, vol. 6, pp. 1097-1105, 2020.
- [19] H. Liu and G. Uhlmann, "Determining both sound speed and internal source in thermo- and photo-acoustic tomography," *Inverse Problems*, vol. 31, no. 10, 2015.
- [20] G. W. Roberts and M. Ali-Bakhshian, "A Brief Introduction to Time-to-Digital and Digital-to-Time Converters," *IEEE Transactions on Circuits and Systems II: Express Briefs*, vol. 57, no. 3, pp. 153-157, 2010.
- [21] M. Xu and L. V. Wang, "Universal back-projection algorithm for photoacoustic computed tomography," *Phys Rev E Stat Nonlin Soft Matter Phys*, vol. 71, no. 1 Pt 2, p. 016706, Jan 2005.
- [22] J. Xiao, X. Luo, K. Peng, and B. Wang, "Improved back-projection method for circular-scanning-based photoacoustic tomography with improved tangential resolution," *Appl Opt*, vol. 56, no. 32, pp. 8983-8990, Nov 10 2017.
- [23] A. Fatima *et al.*, "Review of cost reduction methods in photoacoustic computed tomography," *Photoacoustics*, vol. 15, p. 100137, Sep 2019.